Published in final edited form as:
Langmuir. 2011 May 3; 27(9): 5671–5679. doi:10.1021/la200183x.

Responsive Microgrooves for Formation of Harvestable Tissue Constructs

Halil Tekin[‡,1,2,3], **Gozde Ozaydin-Ince**[‡,4], **Tonia Tsinman**[2], **Karen K. Gleason**[4], **Robert Langer**[*,3,4,5], **Ali Khademhosseini**[*,2,5,6], and **Melik C. Demirel**[*,4,6,7]

[1]Department of Electrical Engineering and Computer Science, Massachusetts Institute of Technology, 77 Massachusetts Avenue, Cambridge, MA, 02139, USA

[2]Department of Medicine, Center for Biomedical Engineering, Brigham and Women's Hospital, Harvard Medical School, Boston, MA 02115, USA

[3]David H. Koch Institute for Integrative Cancer Research, Massachusetts Institute of Technology, Building 76-661, 77 Massachusetts Avenue, Cambridge, MA, 02139, USA

[4]Department of Chemical Engineering, Massachusetts Institute of Technology, Cambridge, MA 02139

[5]Harvard-MIT Division of Health Sciences and Technology, Massachusetts Institute of Technology, Cambridge, MA 02139, USA

[6]Wyss Institute for Biologically Inspired Engineering, Harvard Medical School, Boston, MA, 02138

[7]Materials Research Institute and Department of Engineering Science, Pennsylvania State University, University Park, PA 16802

Abstract

Given its biocompatibility, elasticity and gas permeability, poly(dimethylsiloxane) (PDMS) is widely used to fabricate microgrooves and microfluidic devices for three dimensional (3D) cell culture studies. However, conformal coating of complex PDMS devices prepared by standard microfabrication techniques with desired chemical functionality is challenging. This study describes the conformal coating of PDMS microgrooves with Poly(N-isopropylacrylamide) (PNIPAAm) by using initiated chemical vapor deposition (iCVD). These microgrooves guided the formation of tissue constructs from NIH-3T3 fibroblasts that could be retrieved by the temperature dependent swelling property and hydrophilicity change of the PNIPAAm. The thickness of swollen PNIPAAm films at 24 °C was approximately three times greater than at 37 °C. Furthermore, PNIPAAm coated microgroove surfaces exhibit increased hydrophilicity at 24 °C (contact angle $\theta = 30° \pm 2$) compared to 37 °C ($\theta = 50° \pm 1$). Thus PNIPAAm film on the microgrooves exhibits responsive swelling with higher hydrophilicity at room temperature which could be used to retrieve tissue constructs. The resulting tissue constructs were the same size as the grooves and could be used as modules in tissue fabrication. Given its ability to form and retrieve cell aggregates and its integration with standard microfabrication, PNIPAAm coated PDMS templates may become useful for 3D cell culture applications in tissue engineering and drug discovery.

Prof. Melik C. Demirel - Corresponding-Author (MDemirel@engr.psu.edu), Prof. Ali Khademhosseini - Corresponding-Author (alik@rics.bwh.harvard.edu), Prof. Robert Langer - Corresponding-Author (rlanger@mit.edu).
‡These authors contributed equally to this work.

Keywords

Stimuli-responsive surfaces; poly(dimethylsiloxane); microgrooves; tissue constructs; chemical vapor deposition

Introduction

Poly(dimethylsiloxane) (PDMS) is widely used for fabrication of complex 3D or high aspect ratio microstructures and devices due to its physicochemical properties. Elasticity, ease of processing, biocompatibility, and mechanical stability of PDMS[1] makes it a desirable substrate to fabricate microdevices for biomedical applications such as cell culture[2, 3] and drug toxicity and metabolism screening[4]. Recently, PDMS has been also been used as a stretchable "organ-on-a-chip" device,[5] which could potentially replace expensive animal testing.

PDMS possesses high gas and liquid permeability coefficients due to its large free volume, and low selectivity.[1] Although this may be advantageous for a range of applications, the ability to control the permeability of PDMS surfaces is desirable to prevent the leakage of hydrophobic drugs or metabolites in drug toxicity and metabolism screening. In addition, the ability to reversibly change PDMS substrate properties may be of interest for a range of cell culture applications. Therefore, simple approaches of modifying PDMS substrates while maintaining its mechanical and optical properties are desirable.[6] Strategies for coating pores or microchannels involve vapor phase deposition of crystalline (e.g. parylene[7, 8]) or amorphous polymers (e.g. pHEMA[9]). A crystalline polymer provides a perfect high barrier for molecular penetration but it has limited mechanical properties (e.g. stretchability) due to its high modulus (i.e. elastic modulus of 1-10 GPa). An amorphous polymer, on the other hand, is typically used on stretchable devices to complement the low modulus (i.e. 1-100 MPa) of PDMS but the molecular pores of the amorphous phase should be engineered to gain high barrier properties for moisture as well as chemicals. The latter could be achieved easily, in vapor phase coatings, by adjusting the crosslinker density of the polymer[10].

A few studies have been conducted to fabricate tissue constructs (e.g. cell detachment,[11] mechanical conditioning and cell detachment[12]) using PNIPAAm grafted PDMS[12]. PNIPAAm is a stimuli-response polymer that undergoes a dramatic change in surface energy at its lower critical solution temperature (LCST) of approximately 32 °C. At temperatures above the LCST, PNIPAAm dehydrates, changes its conformation to a collapsed form,[13] which is suitable for cell adhesion and culture at 37 °C. Below LCST, it swells and hydrates in aqueous solution,[13] which drives cell detachment with conditioned ECM from the culture surface without disturbing cell-cell and cell-ECM interactions[14-17]. Surface-grafted PNIPAAm was also used for temperature controlled release of biofilms from the substrates.[18] Thermo-responsive substrates with microgroove patterns were fabricated to form harvestable cell sheets[19] or capillary networks[20]. Microgroove patterns can be potentially useful to align the cells along the channel direction and initiate cytoskeletal organization to form physiologically active modular tissue constructs. In these studies PNIPAAm was grafted in liquid phase on microgrooves to tune surface energy. However, conformal grafting of PNIPAAm in liquid phase was difficult to achieve. Recently, PNIPAAm based hydrogel microstructures were fabricated using a soft lithographic approach, however these microstructures exhibit temperature dependent shape changes which applies mechanical forces on the resulting tissue constructs and may deform the final aggregate shapes[21].

Microtextured surfaces were previously coated with PNIPAAm using electron-beam polymerization in liquid phase.[20] This method has led PNIPAAm to agglomerate non-uniformly in groove patterns and caused rounded shape ridges. Overall process has produced a non-uniform PNIPAAm coating on the substrates which can adversely affect cell orientation and tissue formation within grooves. Herein, we created conformal PNIPAAm coating on PDMS using iCVD technique. iCVD is a free radical polymerization technique to produce structurally well-defined conformal polymer coatings, and therefore offers a high degree of control over the geometry and thickness of the polymer.[10] While traditional grafting approaches require substrates that possess specific functional groups and produce films of limited thickness, the iCVD method can be applied to virtually any substrate and can result in film thicknesses ranging from a few nm to a few microns.[10, 22] The iCVD process occurs in a single step and growth rates can exceed 100 nm/min.[22] We used a growth rate of ~6 nm/min to create ~300 nm conformal PNIPAAm coating on PDMS substrates.

We showed that the conformal coating of PDMS microgrooves with PNIPAAm by using iCVD can be used to form geometrically controlled longitudinal tissue constructs and enable their further retrieval in a temperature dependent manner by exploiting the swelling/deswelling property and tunable hydrophilicity of the responsive polymer. This stimuli-responsive template can be useful in fabricating modular tissue units for tissue engineering applications and potentially integrated within microfluidic devices.

Materials and Methods

Materials

Silicon elastomer and curing agent were purchased from Dow Corning Corporation (Midland, MI). Dulbecco's phosphate buffered saline (PBS), calcein-AM and ethidium homodimer, Dulbecco's modified eagle medium (DMEM), fetal bovine serum (FBS), and penicillin-streptomycin (Pen-strep), Alexa-Fluor 594 Phalloidin were all purchased from Invitrogen (Carlsbad, CA). Glass slides and ethanol were purchased from Fisher Scientific (Fair Lawn, NJ). The monomer, N-Isopropylacrylamide (NIPAAm) (97%), the initiator, Tert-butyl peroxide (TBPO) (98%, Aldrich), trichlorovinylsilane, fluorescein isothiocyanate conjugated bovine serum albumin (FITC-BSA), bovine serum albumin (BSA), TritonX-100 were all purchased from Sigma-Aldrich Chemical Company (St. Louis, MO). Paraformaldehyde was purchased from Electron Microscopy Sciences (Hatfield, PA). The crosslinker, ethylene glycol diacrylate (EGDA) (98%) was purchased from Polysciences Company (Warrington, PA). Silicon (Si) wafers were purchased from University Wafer (Boston, MA).

Fabrication of PDMS microgrooves

Silicon masters with longitudinal patterns were developed with SU-8 photolithography and used as templates to fabricate PDMS replicas. PDMS microgrooves were formed by curing a mixture of 10:1 silicon elastomer and curing agent at 70 °C for 2 h and then detached from silicon masters. The channel depth and width of the resulting PDMS microgrooves were adjusted to ~150 μm. The space between two channels was ~150 μm.

PNIPAAm coating with iCVD

PDMS substrates were treated before iCVD to provide covalent bonding of PNIPAAm to the surface. The PDMS surfaces were first treated with oxygen plasma for 30 seconds. After the plasma treatment the PDMS surfaces were immediately placed in an oven at 40 °C together with 5ml of Trichlorovinylsilane. The samples were kept in the oven for 4 minutes giving them sufficient time to react with silane. Following this treatment the samples were

directly placed in the iCVD reactor for deposition. The iCVD of PNIPAAm were performed in a custom built deposition reactor with a base pressure of 1 mTorr as illustrated in Figure 1a. The monomer and the crosslinker were heated in separate glass jars to 75 °C and 80 °C separately and delivered into the reactor using needle valves. The initiator was kept at room temperature and delivery into the reactor was achieved by using a mass flow controller. Nitrogen gas was used as a patch flow. A filament array of 14 parallel chrome alloy filaments was used for thermal decomposition of the initiator molecules. A back-side cooled sample stage kept the temperature of the sample constant. The thickness of the deposited films was monitored in real-time using a He-Ne laser interferometry set-up, in which the laser beam entered the reactor from the top quartz window and reflected from the sample surface. The thickness measurements were performed on Si-wafers that were located next to PDMS samples in the reactor. The thickness of the film was calculated from the beam intensity oscillations. The iCVD deposition of 300 nm thick PNIPAAm was performed at 100 mTorr pressure and the sample and filament temperatures were kept constant at 30 °C and 250 °C, respectively. The flow rates of NIPAAm, EGDA, TBPO and N_2 were maintained at 5, 1, 1, 1 sccm respectively. At these conditions the growth rate was ~6 nm/min. PNIPAAm reacts with the vinyl bonds of the silane on PDMS surface. Without silane treatment, PNIPAAm can form a conformal thin film without covalent bonding which has weaker adhesion compared to the silanized surface.

Characterization

Surface modification of PNIPAAm deposited PDMS surface was analyzed by Fourier Transform Infrared Spectroscopy with attenuated total reflection (FTIR-ATR). The spectra were recorded by using a Bruker Alpha FTIR. Uncoated PDMS surface was used as control. Chemical characterization of the deposited films on Si-wafer was done using a Nexus 870 FTIR (Thermo Nicolet) equipped with a DTGS-TEC detector. The spectra were acquired at 4 cm^{-1} resolution and the number of scans was kept at 128. The spectrum of a bare Si wafer was used as the background.

Scanning electron microscopy

PNIPAAm coated microgrooves were dried at room temperature. The samples were subsequently mounted onto aluminum stages, sputter coated with gold and analyzed under scanning electron microscopy (SEM) (JEOL JSM 6060) at a working distance of 4 mm.

Atomic Force Microscopy

Surface topography of uncoated and PNIPAAm coated PDMS samples was determined by using an atomic force microscope (AFM) (Nanoscope V, Veeco Inc.). AFM images were obtained in tapping mode using rectangular shaped silicon nitride cantilevers. The root mean square (rms) value of the surface roughness for flattened images was quantified by using the software equipped with Nanoscope V.

Contact angle measurement and swelling test

Static contact angle measurements was performed with deionized water (10 μl droplet) using a contact angle measuring instrument (FTA 1000B, First Ten Angstroms Inc. Portsmouth, VA). To analyze the swelling properties, Si wafers were coated with ~300 nm PNIPAAm, water swelling of the PNIPAAm films was then monitored in real-time using an interferometry set-up (J.A. Woollam Inc., Lincoln, NE).

Cell culture

NIH-3T3 fibroblasts were cultured in medium containing 89% DMEM, 10% FBS, and 1% Penicillin-Streptomycin and passaged every 3 days. Cells were maintained at 37 °C in a 5% CO_2 humidified incubator.

Cell adhesion and protein adsorption on PNIPAAm coated PDMS surfaces

PNIPAAm coated PDMS surfaces, bare PDMS surface, and bare glass slide were rinsed with ethanol, and kept in PBS until cell seeding. NIH-3T3 fibroblasts were trypsinized and prepared in culture medium. All samples were immersed in 6 mL of a cell solution containing 2.5×10^5 cells/mL. Cell adhesion on PNIPAAm coated surfaces were performed at 37 °C for 2 h and 24 °C for 2 h while bare PDMS surface and glass slide were only subjected to 37 °C for 2 h. After incubation at experimental temperatures, all samples were dipped into PBS to remove non-adherent cells. Samples were visualized with an inverted microscope (Nikon Eclipse TE2000-U) and adherent cells were counted.

FITC-BSA was dissolved in PBS at a density of 25 μg/ml. To test the protein adsorption to PNIPAAm coated PDMS surfaces, bare PDMS surface, and bare glass slide, 200 μL of the protein solution was evenly distributed on the surfaces. PNIPAAm coated surfaces were incubated at 37 °C for 2 h and 24 °C for 2 h while bare PDMS surface and glass slide were only subjected to 37 °C for 2 h. After incubation, samples were washed with PBS and analyzed under an inverted fluorescent microscope (Nikon Eclipse TE2000-U). Fluorescent images were analyzed using ImageJ software.

Cell seeding on microgrooves and formation of longitudinal tissues

PNIPAAm coated microgrooves were placed in 6 well culture plates after fabrication, rinsed with ethanol, and kept in PBS until cell seeding. NIH-3T3 fibroblasts were trypsinized and prepared in culture medium. Microgrooves were kept at room temperature for at least 30 min to make the surface hydrophilic for a better cell-seeding condition at 24 °C. After aspirating PBS from each 6 well plate, a suspension of NIH-3T3 fibroblasts was seeded on each microgroove array at a density of $\sim 2.7 \times 10^5$ cells/cm^2 and kept at ambient temperature for 20 min to drive spreading of the cell suspension on the surface. Subsequently, microgroove arrays were gently washed with PBS to remove undocked cells on the microgroove surface and immersed in fresh culture medium. Seeded microgroove arrays were kept in a 5% CO_2 humidified incubator at 37 °C for 3 days. Microscope images were taken daily to analyze longitudinal tissue formation in the microgrooves.

To analyze cytoskeletal organization in microgrooves after 3 days of incubation, F-actin fibrils in the cells within formed tissue constructs were stained with phalloidin. Samples were first fixed with 4% paraformaldehyde for 10 min at room temperature and then rinsed two times with PBS. Cells were permeabilized with 0.1% TritonX-100 for 5 min at room temperature and washed two times with PBS. Samples were then incubated in a PBS solution containing 1% BSA and Alexa-Fluor 594 Phalloidin (1:40 dilution in PBS after dissolving stock powder in 1.5 mL methanol) for 1 h at room temperature. Samples were finally washed three times with PBS and visualized under an inverted fluorescent microscope (Nikon Eclipse TE2000-U).

Live/dead staining

Live/dead solution was prepared with 2 mM of calcein-AM and 4 mM of ethidium homodimer in PBS. For live and dead evaluation, each microgroove was placed in live/dead solution during deposition on a glass substrate for a maximum of 30 min at 24 °C or 37 °C. Live cells were stained by Calcein AM with fluorescent green color while homodimer

stained dead cells with fluorescent red color. Cells were analyzed under an inverted microscope (Nikon Eclipse TE2000-U).

Retrieval of modular longitudinal tissue constructs

After culturing cell-seeded microgroove arrays for 3 days, longitudinal tissue constructs were retrieved from the microgrooves by deposition of the arrays on glass slides as shown in Figure 1c. For release experiments at 24 °C, microgroove arrays (n=3) were gently placed on a glass slide and immersed in 24 °C PBS for 30 min with the grooves facing down. Control experiments for microgroove arrays (n=3) with the same method were performed at 37 °C for 30 min to test whether the temperature was the main driving force in releasing the tissue constructs from the microgrooves. For control experiments at 37 °C, microgrooves were covered with 37 °C PBS. Phase images for each sample were taken using an inverted microscope (Nikon Eclipse TE2000-U). Approximate lengths of retrieved tissue constructs were measured with Spot Advanced software to determine the frequency of tissue lengths for released modular tissue constructs from PNIPAAm coated microgrooves at 24 °C.

Statistical analysis

Data was shown as the mean and ± standard deviation (±sd). Statistical analysis was performed with an unpaired student's t-test and $p < 0.05$ was considered as significant.

Results and Discussion

PNIPAAm coating on PDMS substrates

PNIPAAm coating on PDMS substrates with iCVD method was performed in a custom built deposition reactor as illustrated in Figure 1a. The as-deposited thickness of the responsive film was adjusted to be ~300 nm. The coating thickness on the samples varied ±10 nm, while thickness variation among 4 samples was ± 20 nm. The swelling of the responsive film was observed as illustrated in Figure 1b. To observe the effect of PNIPAAm coating on surface roughness, SEM and tapping mode AFM images were taken for bare PDMS surface (Figure 2a-b) and PNIPAAm coated PDMS surface (Figure 2d-e). Top-view SEM images, AFM images and plots of corresponding height change (Figure 2c and 2f) showing surface topographies demonstrated that PNIPAAm coating on the surface caused increased roughness. RMS values reveal the degree of surface roughness. RMS value of PNIPAAm coated PDMS surface (25.24 nm) is significantly higher than bare PDMS surface surface (1.21 nm), suggesting that PNIPAAm coating on PDMS surfaces were more rough compared to bare PDMS substrates.

We also analyzed the chemical properties of PNIPAAm deposition using FTIR characterization. Figure 3a shows the FTIR spectra of the PNIPAAm coated PDMS surfaces as well as non-coated PDMS substrates. FTIR peaks for the PNIPAAm coated surfaces show O-H stretching at 3700-3050 cm^{-1} for NIPAAm as well as C=O stretching 1750-1690 cm^{-1} for EGDA. Figure 3b shows the FTIR spectra of PNIPAAm deposited Si-wafer. We note that the absence of peaks in Figure 3b due to unsaturated carbon at 1640-1660 cm^{-1} for PNIPAM indicates the complete reaction of the vinyl bonds, thus complete polymerization.

To test the changes in surface energy under temperature transformation from 24 °C and 37 °C, static contact angle measurements were performed for PNIPAAm coated substrates. Interestingly, contact angle at 24 °C was measured to be 30° ± 2, while it was 50° ± 1 at 37 °C. Also, contact angle for bare PDMS surface at 24 °C was measured to be 96° ± 4. It was previously shown that contact angle values for bare PDMS do not change significantly between ambient and physiological temperatures.[23] We also tested the repeatability of temperature dependent wettability of PNIPAAm films at 24 °C and 37 °C. The results

showed a substantial reversibility for 3 cycles of quick temperature transformations between 24 °C and 37 °C (Figure 3c). Furthermore, we observed that volumetric swelling of PNIPAAm film at 24 °C was approximately three times greater than at 37 °C. This observation correlates with recent experiments in which it was shown that PNIPAAm coated Si-wafer with iCVD exhibited 3 times thickness change in swollen state compared to dry state below LCST.[22] Conformal PNIPAAm coating on silicon based substrates demonstrated a significant swelling change and an increased hydrophilicity at room temperature.

Cell adhesion and protein adsorption

To test the cell adhesion on various surfaces, PNIPAAm coated PDMS surfaces, bare PDMS surface, and bare glass slide were immersed in a solution of NIH-3T3 fibroblasts containing 2.5×10^5 cells/mL. Cells adhesion on PNIPAAm coated PDMS surface at 24 °C was significantly less than the control experiments with the same surface and bare PDMS at 37 °C (Figure 4a). Contact angle results indicate that PNIPAAm coated PDMS surfaces had a higher degree of hydrophilicity at 24 °C, which may contribute to a lower level of cell adhesion. It was also previously shown that hydrophilic PNIPAAm surfaces drove the cell detachment from the substrate.[14-17] Another contributing factor to a lower degree of cell adhesion may be due to the increased swelling of the PNIPAAm film on the surface at 24 °C compared to 37 °C. Interestingly, no significant difference was observed between the number of adhered cells to PNIPAAm coated or non-coated PDMS substrates at 37 °C. Both surfaces were hydrophobic at this temperature. Hydrophobic substrates are attractive for protein adsorption and subsequent cell adhesion.[24-29] We hypothesize that the adsorption of proteins such as fibronectin from FBS on hydrophobic surfaces may have caused the same tendency of cell adhesion on these substrates. In addition, cells adhered to glass surface at 37 °C at significantly higher values than all other surfaces.

The protein adsorption on PNIPAAm coated PDMS surfaces, bare PDMS surface, and bare glass slide was analyzed by quantifying the fluorescent expression of these surfaces after exposure to fluorescently labeled protein. As shown in Figure 4b, no significant difference was observed between the degrees of FITC-BSA adsorption on PNIPAAm coated PDMS surface at 24 °C and at 37 °C, although swelling of PNIPAAm film on PDMS surface at 24 °C was more than 37 °C. This suggests that proteins adsorbed on PNIPAAm coatings at both temperatures. Interestingly, protein adsorption at 37 °C on bare PDMS surface was similar to PNIPAAm coated PDMS surface. It was previously reported that proteins may physically adsorb on PDMS with hydrophobic interactions between the protein and PDMS surface.[23] In this study, PNIPAAm film was somewhat swollen at 37 °C. We hypothesize that, for adhesion on PDMS at 37 °C, proteins may have physically adsorbed on PDMS with hydrophobic interactions and in the case of PNIPAAm coated PDMS, proteins may have diffused into PNIPAAm coated PDMS through the somewhat hydrated PNIPAAm chains at 37 °C and adsorbed on PDMS substrate with hydrophobic interactions. We also hypothesize that proteins may have diffused into swollen PNIPAAm film at 24 °C and physically adsorbed onto PDMS layer through hydrophobic interactions. In addition, the fluorescent expression of glass slide at 37 °C was significantly higher than all other substrates.

Cell seeding and formation of longitudinal tissue constructs within PNIPAAm deposited microgrooves

Microfabricated platforms were previously shown to be useful for 3D cell culture with controlled alignment and longitudinal tissue formation.[30-35] This study shows PDMS microgroove patterns functionalized with the deposition of a thermo-responsive polymer and their use in harvestable modular tissue formation. Thermo-responsive films on the microgroove arrays exhibited swelling/deswelling property and had a tunable hydrophilicity

that could be useful in controlling the microgroove surface adhesiveness for tissue formation and retrieval. Cell seeding process plays an important role to immobilize cells inside the grooves and prevent cell growth on the ridges. After fabrication, microgroove arrays were kept at room temperature for 30 min to form a swollen polymer film with increased hydrophilicity before cell seeding at 24 °C to prevent cell adhesion on microgroove surfaces. NIH-3T3 fibroblasts were used as the model cell type to form longitudinal tissues in the channels. To generate tissue constructs in the microgrooves, a suspension of NIH-3T3 fibroblasts were pipetted onto microgroove arrays at a density of ~2.7×10^5 cells/cm^2 at 24 °C. After 20 min incubation at room temperature to drive spreading of cell suspension on microgroove surfaces, arrays were gently rinsed to remove the non-adhered cells that were not inside the microgrooves. As shown in day-0 image of Fig. 5a, there was no cells adhered on the ridges after the cell-seeding process. Cell seeded microgroove arrays were placed in the incubator for 3 days to form longitudinal tissues. Figure 5a shows the cell-seeding efficiency and tissue formation in PNIPAAm deposited microgrooves during the 3 day culture. After one day in culture, tightly packed cell clusters were observed in many microgrooves and by 3 days in culture longitudinal tissue fibers were visible in the majority of the grooves. Similar to two dimensional (2D) cell and protein adhesion experiments, the non-swollen state of the responsive polymer film increases cell adhesion. This contact between cells and the responsive film may increase the stability of the tissue constructs in the microgrooves.

Cell alignment within 3D culture platforms is a crucial element of recreating the tissue complexity of a number of tissues such as muscle.[33, 35] Alignment of the cells were previously achieved with either microfabricated templates[30-34] or patterning methods[35-39]. Herein, we analyzed orientation of the cells within the microgrooves after staining their F-actin fibers with phalloidin. Figure 5b illustrates cytoskeletal organization of the cells within longitudinal tissues after 3 days in culture. In the majority of the microgrooves, F-actin filaments in the cells were aligned along the direction of the grooves. Actin fiber intensity and organization show well oriented and interconnected cells within microtissues, suggesting that PNIPAAm deposited templates can be potentially useful to form tissue constructs with controlled alignment and cytoskeletal organization.

Retrieval of tissue constructs from PNIPAAm deposited microgrooves

Retrieval of longitudinal tissues is a desirable property of microfabricated culture templates. This study describes a temperature responsive strategy for tissue retrieval from PNIPAAm deposited PDMS microgrooves by exploiting swelling/deswelling property and hydrophilicity change of responsive polymer film on the substrate. As shown in Figure 1c, for the retrieval of micro tissues, glass slides were gently placed on the microgroove arrays, and the entire structures were flipped to initiate the detachment of tissue constructs through gravity. Inverted microgrooves were covered with PBS to keep PNIPAAm film in an aqueous environment. Retrieval experiments were performed at 24 °C and 37 °C. Microgroove arrays were incubated for 30 min at particular temperature while they were placed face down on a glass slide. After a 30 min incubation, excess solution was removed from the periphery and the microgroove arrays were gently detached from the glass surface as shown in Figure 1c.

When the retrieval experiment was performed at 37 °C, with PNIPAAm film on the surface in a hydrophilic and less swollen state, no tissue retrieval was observed from PNIPAAm deposited microgrooves (Figure 6a). In these experiments only a few individual cells were detached from the arrays as shown in Figure 6a. However, when the procedure was conducted at 24 °C while the PNIPAAm film was in a more hydrophilic and swollen state, microgrooves demonstrated a dramatic increase in retrieval of longitudinal tissues (Figure 6b). Furthermore, we observed high cell viability levels based live/dead staining images for

retrieval experiments that were conducted at 24 °C (Figure 6c), suggesting that neither PNIPAAm film deposited on the substrate nor retrieval process did not adversely affect the cell viability.

Comparison between the results of control experiments at 37 °C and results of retrieval experiments at 24 °C and considering microgrooves flipped through gravity at both temperatures suggest that swelling and hydrophilicity change of PNIPAAm film on the substrate at two different temperatures is the main cause for the retrieval of the modular tissues. We hypothesize that higher hydrophilicity of the PNIPAAm film at 24 °C makes the surface undesirable for cell adhesion and initiates cell detachment and swelling of the PNIPAAm film at 24 °C compared to 37 °C changes the topography of the surface which can drive subsequent release of tissue constructs from the grooves. During retrieval experiments at 24 °C and at 37 °C, microgroove arrays were placed in an aqueous environment. Although the aqueous solution was removed before the detachment of the arrays from the glass surface, there was liquid remaining underneath the microgrooves. The detachment of the arrays from the deposition substrates may have initiated a liquid flow which may subsequently have caused hydrodynamic forces. We infer that release of singles cells at 37 °C was resulted from these hydrodynamic forces. These forces may have disrupted the cells which were not well interconnected with tissue structures because of less cell-cell and cell-ECM contacts.

To characterize the uniformity of the retrieved modular tissues, the lengths of the retrieved tissue constructs were quantified. A wide distribution in the frequency of lengths of longitudinal tissues was observed, as shown in Figure 6d. This may be due to the hydrodynamic forces in aqueous environment occurred during the detachment of microgroove arrays from the deposition surface or due to less cell-cell and cell-ECM interactions. These modular tissues can be convenient models for cardiac tissues[37], myotubes[40], myocardium tissues[32], skeletal muscle tissues[34], and capillaries[20]. In further studies, using modular tissue engineering methods[41], it may be possible to assemble these modular tissue units into defined geometries to form more elaborate tissue constructs.

Harvesting tissue constructs from culture platforms with either digestive enzymes or mechanical scraping often causes undesirable effects on cells and their conditioned ECM.[19, 42, 43] PNIPAAm grafted culture substrates were previously used to form tissue structures and detach them from the culture surface by using switchable hydrophilicity/hydrophobicity at two different temperatures.[19, 20] However, previous coating method on microstructured substrates led to non-conformal PNIPAAm coatings.[19, 20] In this study, PNIPAAm coating with iCVD caused a conformal thin film on PDMS microgrooves which provided a desirable 3D microenvironment for structural organization of the cells to form tissue fibers. In addition, conformally coated rigid PDMS substrates provide an advantage over soft-lithographically fabricated PNIPAAm microstructures[21] in terms of stability under temperature changes because temperature dependent shape changing characteristics of soft-lithographically fabricated PNIPAAm microstructures apply mechanical forces on cell aggregates and may cause deformation on resulting tissue structures[21]. Furthermore, responsive polymer film exhibited a remarkable swelling change and an increased hydrophilicity at 24 °C compared to 37 °C. This swollen state and increased hydrophilicity of the polymer film caused subsequent retrieval of modular tissue constructs from the grooves. These properties suggest that PNIPAAm deposited PDMS microgrooves may be useful as 3D culture platforms.

Conclusion

In summary, conformal coating of PNIPAAm on the PDMS microgroove substrates is shown. We demonstrated that these responsive microgrooves can generate tissue fibers and enable their subsequent release in a temperature dependent manner. Temperature responsive film on the templates exhibited more swelling and higher hydrophilicity at room temperature compared to physiological temperature. Furthermore, the swollen state PNIPAAm film with increased hydrophilicity at room temperature initiated the retrieval of modular tissue constructs. This stimuli-responsive template can be potentially integrated with microfluidic devices and may become a versatile tool for various applications that require modular tissue formation and experimentation, such as tissue engineering and drug discovery.

Acknowledgments

We would like to thank financial supports from the U.S. Army Research Office through the Institute for Soldier Nanotechnologies at MIT under the project DAAD-19-02-D-002, the Draper Laboratory, the NIH(DE01323, DE016516, HL092836, DE019024, EB007249), the NSF Career Award (DMR0847287), the Wyss Institute for Biologically Inspired Engineering, and the Office of Naval Research Young Investigator Award.

References

1. Peppas NA, Langer R. New Challenges in Biomaterials. Science. 1994; (5154):1715–1720. [PubMed: 8134835]
2. Hung PJ, Lee PJ, Sabounchi P, Aghdam N, Lin R, Lee LP. A novel high aspect ratio microfluidic design to provide a stable and uniform microenvironment for cell growth in a high throughput mammalian cell culture array. Lab on a Chip. 2005; 5(1):44–48. [PubMed: 15616739]
3. Kim MS, Yeon JH, Park JK. A microfluidic platform for 3-dimensional cell culture and cell-based assays. Biomedical Microdevices. 2007; 9(1):25–34. [PubMed: 17103048]
4. Ye NN, Qin JH, Shi WW, Liu X, Lin BC. Cell-based high content screening using an integrated microfluidic device. Lab on a Chip. 2007; 7(12):1696–1704. [PubMed: 18030389]
5. Huh D, Matthews BD, Mammoto A, Montoya-Zavala M, Hsin HY, Ingber DE. Reconstituting Organ-Level Lung Functions on a Chip. Science. 2010; 328(5986):1662–1668. [PubMed: 20576885]
6. Lee JN, Park C, Whitesides GM. Solvent compatibility of poly(dimethylsiloxane)-based microfluidic devices. Analytical Chemistry. 2003; 75(23):6544–6554. [PubMed: 14640726]
7. Wright D, Rajalingam B, Karp JM, Selvarasah S, Ling YB, Yeh J, Langer R, Dokmeci MR, Khademhosseini A. Reusable, reversibly sealable parylene membranes for cell and protein patterning. Journal of Biomedical Materials Research Part A. 2008; 85A(2):530–538. [PubMed: 17729252]
8. Demirel G, Malvadkar N, Demirel MC. Template-based and template-free preparation of nanostructured parylene via oblique angle polymerization. Thin Solid Films. 2010; 518(15):4252–4255.
9. Ince GO, Demirel G, Gleason KK, Demirel MC. Highly swellable free-standing hydrogel nanotube forests. Soft Matter. 2010; 6(8):1635–1639.
10. Alf ME, Asatekin A, Barr MC, Baxamusa SH, Chelawat H, Ozaydin-Ince G, Petruczok CD, Sreenivasan R, Tenhaeff WE, Trujillo NJ, Vaddiraju S, Xu JJ, Gleason KK. Chemical Vapor Deposition of Conformal, Functional, and Responsive Polymer Films. Advanced Materials. 2010; 22(18):1993–2027. [PubMed: 20544886]
11. Ma D, Chen HW, Shi DY, Li ZM, Wang JF. Preparation and characterization of thermo-responsive PDMS surfaces grafted with poly(N-isopropylacrylamide) by benzophenone-initiated photopolymerization. Journal of Colloid and Interface Science. 2009; 332(1):85–90. [PubMed: 19168188]
12. Lee EL, von Recum HA. Cell culture platform with mechanical conditioning and nondamaging cellular detachment. Journal of Biomedical Materials Research Part A. 2010; 93A(2):411–418. [PubMed: 20358641]

13. Okano T, Yamada N, Okuhara M, Sakai H, Sakurai Y. Mechanism of Cell Detachment from Temperature-Modulated, Hydrophilic-Hydrophobic Polymer Surfaces. Biomaterials. 1995; 16(4): 297–303. [PubMed: 7772669]

14. Canavan HE, Cheng XH, Graham DJ, Ratner BD, Castner DG. Surface characterization of the extracellular matrix remaining after cell detachment from a thermoresponsive polymer. Langmuir. 2005; 21(5):1949–1955. [PubMed: 15723494]

15. Canavan HE, Cheng XH, Graham DJ, Ratner BD, Castner DG. Cell sheet detachment affects the extracellular matrix: A surface science study comparing thermal liftoff, enzymatic, and mechanical methods. Journal of Biomedical Materials Research Part A. 2005; 75A(1):1–13. [PubMed: 16086418]

16. Kushida A, Yamato M, Kikuchi A, Okano T. Two-dimensional manipulation of differentiated Madin-Darby canine kidney (MDCK) cell sheets: The noninvasive harvest from temperature-responsive culture dishes and transfer to other surfaces. Journal of Biomedical Materials Research. 2001; 54(1):37–46. [PubMed: 11077401]

17. Kushida A, Yamato M, Konno C, Kikuchi A, Sakurai Y, Okano T. Decrease in culture temperature releases monolayer endothelial cell sheets together with deposited fibronectin matrix from temperature-responsive culture surfaces. Journal of Biomedical Materials Research. 1999; 45(4): 355–362. [PubMed: 10321708]

18. Ista LK, Perez-Luna VH, Lopez GP. Surface-grafted, environmentally sensitive polymers for biofilm release. Applied and Environmental Microbiology. 1999; 65(4):1603–1609. [PubMed: 10103257]

19. Isenberg BC, Tsuda Y, Williams C, Shimizu T, Yamato M, Okano T, Wong JY. A thermoresponsive, microtextured substrate for cell sheet engineering with defined structural organization. Biomaterials. 2008; 29(17):2565–2572. [PubMed: 18377979]

20. Tsuda Y, Yamato M, Kikuchi A, Watanabe M, Chen GP, Takahashi Y, Okano T. Thermoresponsive microtextured culture surfaces facilitate fabrication of capillary networks. Advanced Materials. 2007; 19(21):3633–3636.

21. Tekin H, Anaya M, Brigham MD, Nauman C, Langer R, Khademhosseini A. Stimuli-responsive microwells for formation and retrieval of cell aggregates. Lab Chip. 2010; 10(18):2411–2418. [PubMed: 20664846]

22. Alf ME, Godfrin PD, Hatton TA, Gleason KK. Sharp Hydrophilicity Switching and Conformality on Nanostructured Surfaces Prepared via Initiated Chemical Vapor Deposition (iCVD) of a Novel Thermally Responsive Copolymer. Macromolecular Rapid Communications. 2010; 31(24):2166–2172. [PubMed: 21567647]

23. Sugiura S, Imano W, Takagi T, Sakai K, Kanamori T. Thermoresponsive protein adsorption of poly(N-isopropylacrylamide)-modified streptavidin on polydimethylsiloxane microchannel surfaces. Biosensors & Bioelectronics. 2009; 24(5):1135–1140. [PubMed: 18678482]

24. Lydon MJ, Minett TW, Tighe BJ. Cellular Interactions with Synthetic-Polymer Surfaces in Culture. Biomaterials. 1985; 6(6):396–402. [PubMed: 4084641]

25. Baier RE, Meyer AE, Natiella JR, Natiella RR, Carter JM. Surface-Properties Determine Bioadhesive Outcomes - Methods and Results. Journal of Biomedical Materials Research. 1984; 18(4):337–355.

26. Schakenraad JM, Busscher HJ, Wildevuur CRH, Arends J. The Influence of Substratum Surface Free-Energy on Growth and Spreading of Human-Fibroblasts in the Presence and Absence of Serum-Proteins. Journal of Biomedical Materials Research. 1986; 20(6):773–784. [PubMed: 3722214]

27. Klebe RJ, Bentley KL, Schoen RC. Adhesive Substrates for Fibronectin. Journal of Cellular Physiology. 1981; 109(3):481–488. [PubMed: 7320060]

28. Pettit DK, Horbett TA, Hoffman AS. Influence of the Substrate Binding Characteristics of Fibronectin on Corneal Epithelial-Cell Outgrowth. Journal of Biomedical Materials Research. 1992; 26(10):1259–1275. [PubMed: 1429748]

29. Yamato M, Konno C, Kushida A, Hirose M, Utsumi M, Kikuchi A, Okano T. Release of adsorbed fibronectin from temperature-responsive culture surfaces requires cellular activity. Biomaterials. 2000; 21(10):981–986. [PubMed: 10768749]

30. Charest JL, Garcia AJ, King WP. Myoblast alignment and differentiation on cell culture substrates with microscale topography and model chemistries. Biomaterials. 2007; 28(13):2202–2210. [PubMed: 17267031]

31. Motlagh D, Hartman TJ, Desai TA, Russell B. Microfabricated grooves recapitulate neonatal myocyte connexin43 and N-cadherin expression and localization. Journal of Biomedical Materials Research Part A. 2003; 67A(1):148–157. [PubMed: 14517872]

32. Camelliti P, Gallagher JO, Kohl P, McCulloch AD. Micropatterned cell cultures on elastic membranes as an in vitro model of myocardium. Nature Protocols. 2006; 1(3):1379–1391.

33. Kim DH, Lipke EA, Kim P, Cheong R, Thompson S, Delannoy M, Suh KY, Tung L, Levchenko A. Nanoscale cues regulate the structure and function of macroscopic cardiac tissue constructs. Proceedings of the National Academy of Sciences of the United States of America. 2010; 107(2): 565–570. [PubMed: 20018748]

34. Bian WN, Liau B, Badie N, Bursac N. Mesoscopic hydrogel molding to control the 3D geometry of bioartificial muscle tissues. Nature Protocols. 2009; 4(10):1522–1534.

35. Aubin H, Nichol JW, Hutson CB, Bae H, Sieminski AL, Cropek DM, Akhyari P, Khademhosseini A. Directed 3D cell alignment and elongation in microengineered hydrogels. Biomaterials. 2010; 31(27):6941–6951. [PubMed: 20638973]

36. Karp JM, Yeo Y, Geng WL, Cannizarro C, Yan K, Kohane DS, Vunjak-Novakovic G, Langer RS, Radisic M. A photolithographic method to create cellular micropatterns. Biomaterials. 2006; 27(27):4755–4764. [PubMed: 16730059]

37. Khademhosseini A, Eng G, Yeh J, Kucharczyk PA, Langer R, Vunjak-Novakovic G, Radisic M. Microfluidic patterning for fabrication of contractile cardiac organoids. Biomedical Microdevices. 2007; 9(2):149–157. [PubMed: 17146728]

38. Chen CS, Mrksich M, Huang S, Whitesides GM, Ingber DE. Geometric control of cell life and death. Science. 1997; 276(5317):1425–1428. [PubMed: 9162012]

39. Mooney D, Hansen L, Vacanti J, Langer R, Farmer S, Ingber D. Switching from Differentiation to Growth in Hepatocytes - Control by Extracellular-Matrix. Journal of Cellular Physiology. 1992; 151(3):497–505. [PubMed: 1295898]

40. Huang NF, Patel S, Thakar RG, Wu J, Hsiao BS, Chu B, Lee RJ, Li S. Myotube assembly on nanofibrous and micropatterned polymers. Nano Letters. 2006; 6(3):537–542. [PubMed: 16522058]

41. Nichol JW, Khademhosseini A. Modular tissue engineering: engineering biological tissues from the bottom up. Soft Matter. 2009; 5(7):1312–1319. [PubMed: 20179781]

42. Kikuchi A, Okano T. Nanostructured designs of biomedical materials: Applications of cell sheet engineering to functional regenerative tissues and organs. Journal of Controlled Release. 2005; 101(1-3):69–84. [PubMed: 15588895]

43. Von Recum HA, Okano T, Kim SW, Bernstein PS. Maintenance of retinoid metabolism in human retinal pigment epithelium cell culture. Experimental Eye Research. 1999; 69(1):97–107. [PubMed: 10375454]

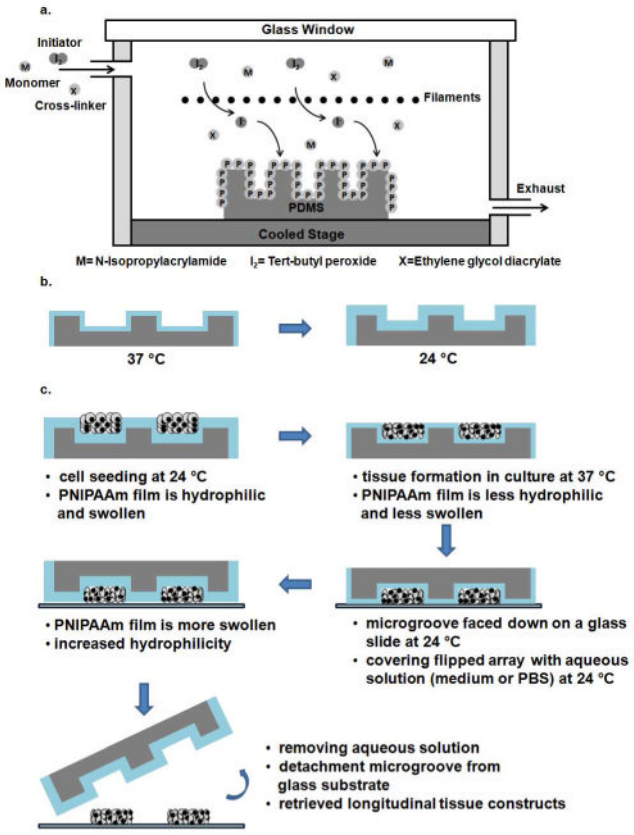

Figure 1.

Schematic of a) PNIPAAm coating on PDMS microgrooves by chemical vapor deposition. b) Swelling of PNIPAAm film on PDMS microgrooves at physiological (37 °C) and ambient temperature (24 °C). c) Formation and retrieval process of longitudinal tissue constructs.

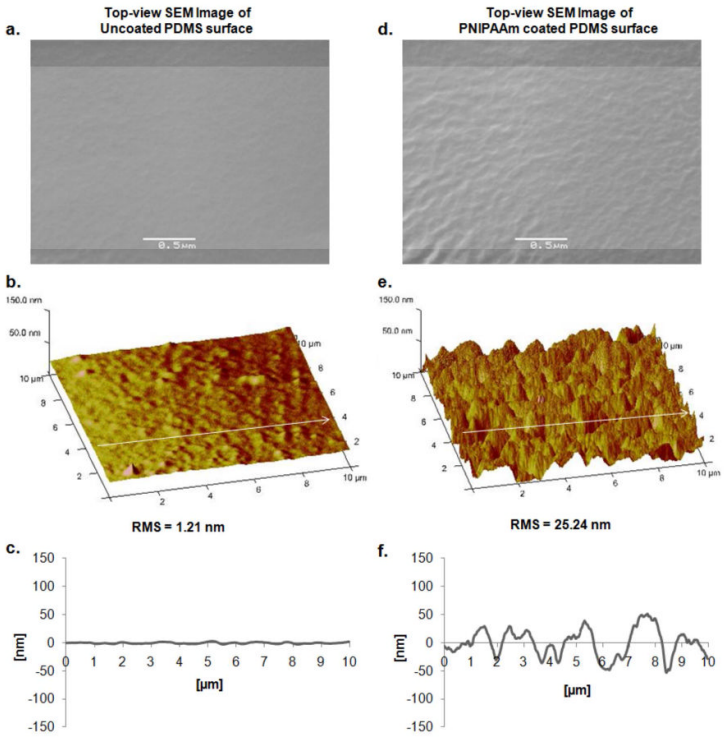

Figure 2.

a) Scanning electron microscopy image and **b)** Atomic force microscopy image showing surface topography of uncoated PDMS surface. Surface analysis for flattened AFM image of bare PDMS surface gives RMS value of 1.21 nm. **c)** Height change for uncoated PDMS surface through arrow direction. **d)** Scanning electron microscopy image and **e)** AFM image showing surface topography of PNIPAAm coated PDMS surface. Surface analysis for PNIPAAm coated PDMS surface exhibits RMS value of 25.24 nm. **f)** Height change over the topography of PNIPAAm coated PDMS surface through arrow direction.

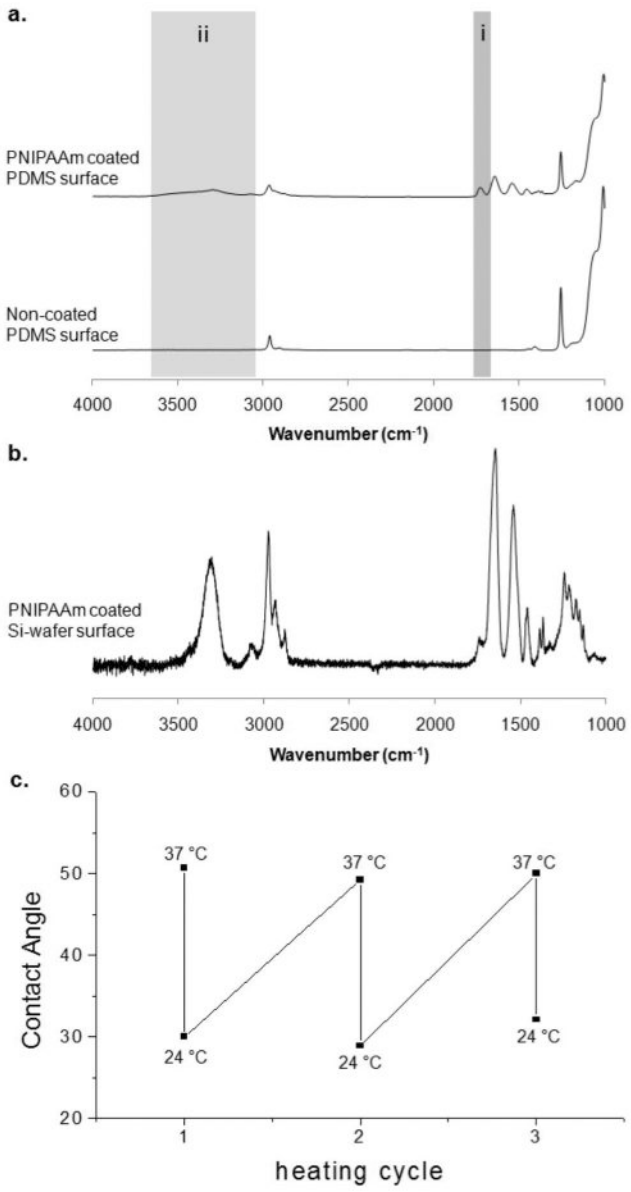

Figure 3.

a) The FTIR spectra for iCVD PNIPAAm on PDMS (top) and bare PDMS (bottom). The shaded regions correspond to (i) C=O stretching at 1750-1690 cm^{-1} for EGDA and (ii) O-H stretching at 3700-3050 cm^{-1} for NIPAAm. Additionally, the amide I (~1660 cm^{-1}) and amide II (~1530 cm^{-1}) bands are visible in both iCVD coated PDMS and in **b)** FTIR spectra for iCVD PNIPAAm on a Si-wafer substrate. The absence of peaks due to unsaturated carbon at 1640-1660 cm^{-1} for PNIPAM shows the complete reaction of the vinyl bonds. **c)** Contact angle results for PNIPAAm film for 3 cycles of quick temperature changes between 24 °C and 37 °C.

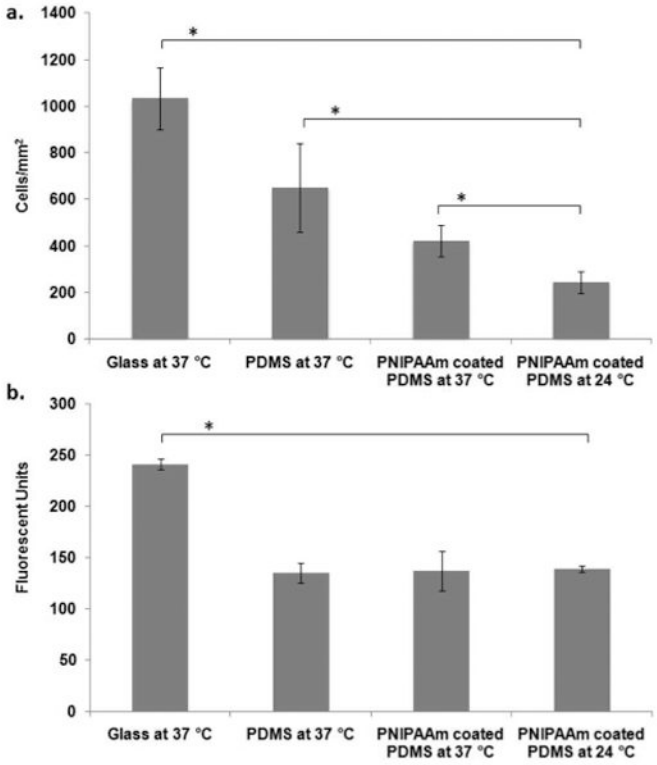

Figure 4.

a) Cell adhesion and **b)** Protein adsorption on 300 nm of PNIPAAm coated 2D PDMS surfaces for 2h incubation at 37 °C and at 24 °C and comparison with adhesion on bare PDMS and glass surfaces. * shows statistically significant difference in variance ($p < 0.05$).

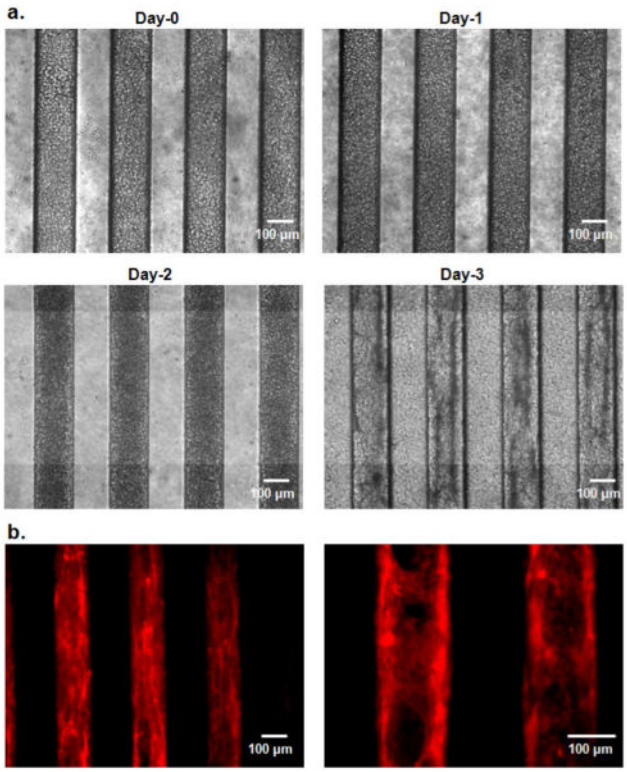

Figure 5.
a) Seeding NIH-3T3 cells onto PNIPAAm coated microgrooves and formation of longitudinal tissue constructs. **b)** Phalloidin staining to visualize F-actin in tissue constructs formed within PNIPAAm coated microgrooves by day 3.

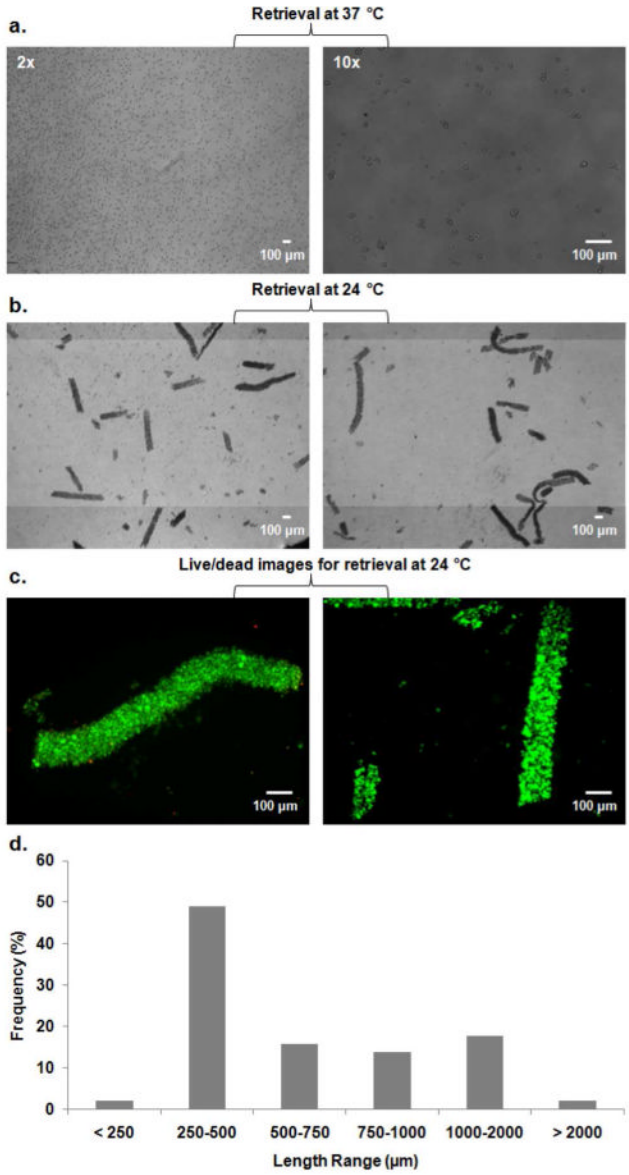

Figure 6.

Retrieval of longitudinal tissue constructs from PNIPAAm coated microgrooves on a glass slide **a)** Phase and live/dead images for control experiment at 37 °C show that only single cells were detached from PNIPAAm coated microgrooves. **b)** Low magnification (2×) phase contrast images of retrieved tissues from PNIPAAm microgrooves after incubation at 24 °C. **c)** Fluorescent images of tissue constructs with live/dead staining. **d)** Frequency of lengths of longitudinal tissues retrieved from PNIPAAm coated microgrooves at 24 °C.